Journal of ELECTRONIC MATERIALS, Vol. 40, No. 5, 2011
DOI: 10.1007/s11664-010-1474-z

Thermoelectric Properties of Co-Doped TiS_2

J. ZHANG,[1] X.Y. QIN,[1,2] H.X. XIN,[1] D. LI,[1] and C.J. SONG[1]

1.—Key Laboratory of Materials Physics, Institute of Solid State Physics, Chinese Academy of Sciences, Hefei 230031, People's Republic of China. 2.—e-mail: xyqin@issp.ac.cn

The thermoelectric properties of cobalt-doped compounds $Co_xTi_{1-x}S_2$ ($0 \le x \le 0.3$) prepared by solid-state reaction were investigated from 5 K to 310 K. It was found that the electric resistivity ρ and absolute thermopower $|S|$ for all the doped compounds decreased significantly with increasing Co content over the whole temperature range investigated. The increased lattice thermal conductivity of the doped compounds would imply enhancement of the acoustic velocity. Moreover, the ZT value of the doped compounds was improved over the whole temperature range investigated, and specifically reached 0.03 at 310 K for $Co_{0.3}Ti_{0.7}S_2$, being about 66% larger than that of TiS_2.

Key words: Thermoelectric, thermal conductivity, resistivity, TiS_2

INTRODUCTION

TiS_2 has an anisotropic structure with a trigonal space group, $P\bar{3}m1$. It is known to exist in two polytypes ($1T$, $2H$) with octahedral and trigonal-prismatic coordinations, respectively. The main difference between the $1T$-TiS_2 and $2H$-TiS_2 layers is the type of local coordination of the metal: octahedral ($1T$) versus trigonal-prismatic ($2H$)[1] (Fig. 1). The most stable form of TiS_2 ($1T$-TiS_2, crystallizing in a layered CdI_2-like structure) consists of sheets of face-sharing TiS_6 octahedra forming S-Ti-S sandwich layers, where a Ti sheet is sandwiched between two sulfur sheets. Atoms within S-Ti-S sheets are bound by strong covalent interactions, whereas bonding between the layers is determined by weak, van der Waals forces.

Although the structure of TiS_2 is quite simple, the nature of the electronic structure of layered TiS_2 has been in dispute over the past decades. To date, for instance, whether it is a semiconductor or semimetal has not been clarified.[2–16] Through measurements of the Hall coefficient, Seebeck coefficient, and resistivity as a function of pressure, Klipstein and Friend[2] found that the band overlap between S 3p states and Ti 3d states increased at a rate of 4.5 meV/kbar, and concluded that TiS_2 is a semiconductor with a gap of 0.18 ± 0.06 eV. The optical measurements of Greenway and Nische[3] indicated that TiS_2 is a semiconductor with a gap of 1 eV to 2 eV. Chen et al.[4] and Barry et al.[5] reported a band gap of about 0.3 eV from angle-resolved photoemission studies (ARPS). Photoemission experiments by Shepherd and Williams[6] indicate a band gap of less than 0.5 eV, and calculations using the pseudopotential (PP) method[7] indicated that TiS_2 is a semiconductor with an indirect band gap of about 2 eV. On the contrary, some theoretical calculations indicate that TiS_2 is a semimetal. Lately, Benesh et al.[8] obtained a semimetallic ground state for TiS_2 by using the linearized augmented plane wave (LAPW) method as a function of pressure. Similarly, band calculations based on the augmented spherical wave (ASW) method by Fang et al.,[9] the linear muffin-tin orbital (LMTO) method by Wu et al.,[10–12] and the full-potential (FP)-LAPW method[13,14] showed that TiS_2 possessed a semimetallic ground state. Meanwhile, many experiments[15,16] have indicated that the electrical resistivity of TiS_2 almost exclusively exhibits metallic behavior, decreasing with decreasing temperature down to nearly 0 K. To date, no semiconductor behavior in the conductivity of TiS_2 has ever been observed experimentally. Hence, it is interesting and also significant (as mentioned below) to clarify the observed contradictory phenomena concerning the properties of TiS_2.

On the other hand, layer-structured TiS_2 is well known for its capability for intercalation by a wide range of both organic and inorganic materials into its van der Waals gap.[17] Since Li^+ can easily intercalate into and leave the van der Waals gap of

(Received April 29, 2010; accepted November 29, 2010; published online January 4, 2011)

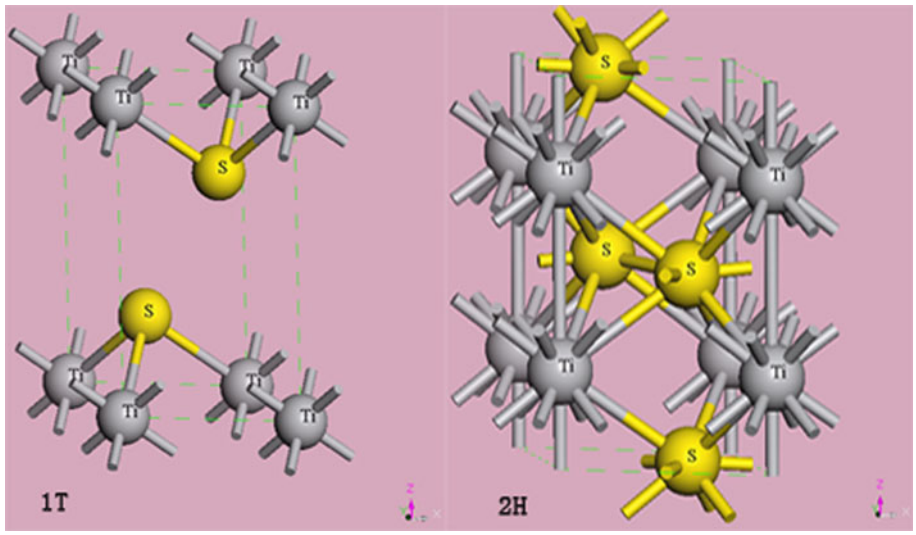

Fig. 1. Crystal structures of TiS_2 with 1*T* (*left*) and 2*H* (*right*) structure.

TiS_2, TiS_2 has been studied as a promising cathode material for rechargeable lithium-ion batteries.[17–19] Besides Li,[2,20,21] transition metals, such as Fe, Co, and Ni,[22] have been successfully inserted into the gap of TiS_2, and the influence of such intercalation on the physical properties of the corresponding compounds has been investigated and explored. Specifically, Imai et al. reported that TiS_2 has a large thermopower of $S = 251\ \mu V/K$ and a power factor of $S^2/\rho = 37.1\ \mu W/cm\ K^2$ (where ρ is the electrical resistivity) at room temperature,[23] indicating that TiS_2 is a potential candidate for thermoelectric applications. Very recently, work in our group indicated that a large enhancement of the thermoelectric properties for TiS_2 can be realized by proper Bi intercalation into its van der Waals gap.[24]

As outlined above, to tailor or improve the physical properties of TiS_2, the numerous works conducted so far have concentrated mainly on intercalation of guest atoms or molecules. The aim of the present work is to synthesize the cobalt-doped compounds $Co_xTi_{1-x}S_2$ and to investigate the effect of Co doping (substitution for Ti and intercalation in the van der Waals gap of TiS_2) on their transport properties and thermoelectric performance in the temperature range from 5 K to 310 K. Our results show that Co doping could not only cause significant changes of the transport properties but also give rise to enhancement of the thermoelectric performance of TiS_2 when doped properly.

EXPERIMENTAL PROCEDURES

Polycrystalline samples of the cobalt-substituted compounds $Co_xTi_{1-x}S_2$ with nominal x values of 0, 0.05, 0.075, 0.10, 0.20, and 0.30 were prepared by a solid-state reaction method. Elementary cobalt (99.9 wt.%), titanium (99.99 wt.%), and sulfur (99.999 wt.%) powders were weighed accurately to give the desired composition, mixed intimately to give a homogeneous mixture, and sealed in an evacuated quartz tube, which was heat-treated in a horizontal furnace at 880 K for 7 days at a fixed heating rate of 0.5 K/min. The compounds obtained were ground in an agate mortar to fine powders, which were then compacted by hot-pressing (under pressure of 300 MPa) in vacuum at 673 K for 1 h to form bulk samples with dimensions of 10 mm × 30 mm × (2 mm to 3 mm). To measure the thermoelectric properties, bar-shaped specimens with dimensions of 12 mm × 3 mm × ~2 mm were cut from the bulk samples.

The phase structures and compositions of the samples obtained were verified using x-ray powder diffraction (XRD), carried out using a Philips diffractometer with Cu K_α radiation. Accurate lattice parameters were determined from the d-values of the XRD peaks using a standard least-squares refinement method with a Si standard for calibration. Measurements of transport properties [direct-current (DC) resistivity, thermal conductivity, and thermopower] were carried out using a physical property measurement system (PPMS; Quantum Design) in the temperature range from 5 K to 310 K.

RESULTS AND DISCUSSION

Phase Determination and Change of Lattice Parameters After Co Doping Analyzed by X-Ray Diffraction

Figure 2 shows XRD patterns for the synthesized specimens with different Co contents x. One can see from Fig. 2 that all the main peaks of the XRD patterns match well with those for TiS_2, indicating that the doped specimens have the same crystallographic structure as that of TiS_2, despite

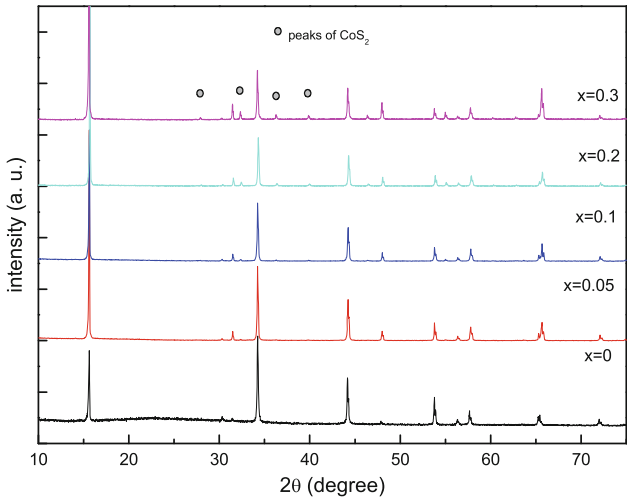

Fig. 2. XRD patterns of Co-doped compounds $Co_xTi_{1-x}S_2$ with (a) $x = 0$, (b) $x = 0.05$, (c) $x = 0.10$, (d) $x = 0.20$, and (e) $x = 0.30$.

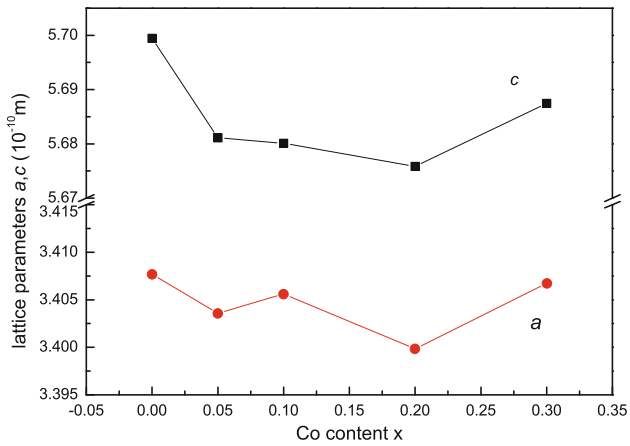

Fig. 3. Variation of the lattice parameters a and c with Co content x.

some peaks of CoS_2 occurring with increasing Co content for $x > 0.1$. The values of the lattice parameters a and c for all the samples were calculated from the XRD data and are presented in Fig. 3. It can be seen that the lattice parameter c decreases rapidly from 5.6965 Å to 5.6758 Å with increasing cobalt content x from 0 to 0.20, then the parameter c increases to 5.68745 Å as the cobalt content increases further to $x = 0.30$. Similarly, the lattice parameter a decreases firstly from 3.4077 Å to 3.3998 Å as the cobalt content x increases from 0 to 0.20, and then a increases to 3.4067 Å for $x = 0.30$. Many investigations[25–28] have shown that the lattice parameter a of the intercalated compounds M_yTiS_2 (where M stands for intercalated elements) is always found to increase with increasing content of intercalated elements. (For example, the lattice parameter a changed from 3.4083 Å to 3.4156 Å in Bi_yTiS_2[25] with y increasing from 0 to 0.25; the parameter a of Li_yTiS_2[27] changed from 3.407 Å to 3.452 Å with increasing y from 0 to 1.0; the parameter a of self-intercalated compound $Ti_{1+y}S_2$[28] increased from 3.405 Å to 3.412 Å with y increasing from 0 to 0.1; see Table I.) Other research has indicated that the parameter a decreases as other atoms are substituted for Ti atoms; for example, the lattice parameter a changed from 3.4098 Å to 3.4038 Å in $Mg_xTi_{1-x}S_2$[29] with x increasing from 0 to 0.04; the parameter a of $Cd_xTi_{1-x}S_2$[30] changed from 3.4098 Å to 3.4044 Å with increasing y from 0 to 0.025. Therefore, the decrease of parameters a and c reflects that substitution of Co (for Ti) has occurred after Co addition, as the atomic radius of cobalt is smaller than that of Ti, and if Co atoms replace Ti atoms to form covalent bonds[31] the lattice of $Co_xTi_{1-x}S_2$ will shrink compared with that of TiS_2. However, the increase in the parameters a and c for a cobalt content $x > 0.2$ suggests that some of the Co atoms possibly intercalated into the van der Waals gap of TiS_2 in heavily doped compounds, accompanying Co substitution for Ti, which can be verified by their DC resistivity as discussed in the next section.

Effects of Co Doping on DC Resistivity

The temperature dependence of the electrical resistivity for specimens with different Co contents is shown in Fig. 4, which shows that the resistivity of all doped compounds was smaller than that of pure TiS_2. One can see that the ρ–T curve for the pure TiS_2 sample ($x = 0$) shows metal-like behavior (i.e., $d\rho/dT > 0$) over the whole temperature range investigated. Fitting the resistivity to a power law, $[\rho(T) - \rho_0] \propto T^{\gamma}$, gives $\gamma = 2.2$, in agreement with

Table I. Lattice parameter a (Å) of several intercalated and substituted compounds[25,27–30]

y or x	Bi_yTiS_2	Li_yTiS_2	$Ti_{1+y}S_2$	$Mg_xTi_{1-x}S_2$	$Cd_xTi_{1-x}S_2$	$Co_xTi_{1-x}S_2$
0	3.4083	3.407	3.405	3.4098	3.4098	3.4077
0.025	3.4097	–	–	–	3.4044	–
0.04	–	–	–	3.4038	–	–
0.05	3.4111	–	–	–	3.4039	3.4036
0.1	3.4122	–	3.412	–	–	3.4056
0.20	3.4156	–	–	–	–	3.3998
1.0	–	3.452	–	–	–	–

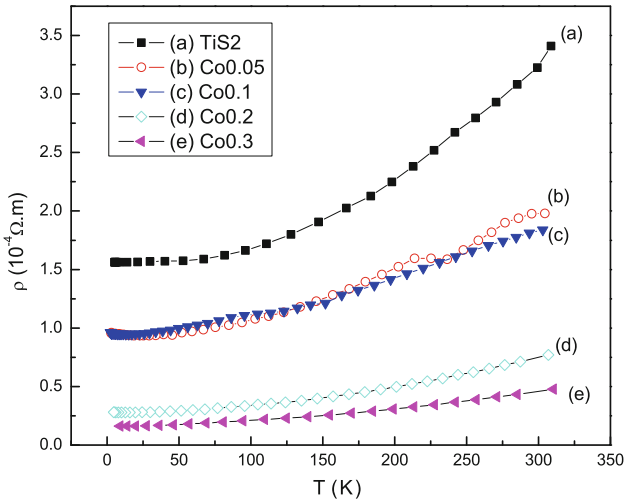

Fig. 4. Dependence of the electrical resistivity ρ on temperature for Co-doped compounds $Co_xTi_{1-x}S_2$ with (a) $x = 0$, (b) $x = 0.05$, (c) $x = 0.10$, (d) $x = 0.20$, and (e) $x = 0.30$.

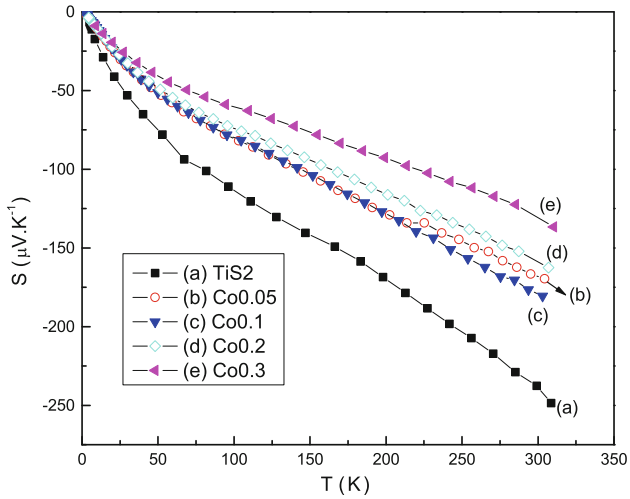

Fig. 5. Variation of thermopower S with temperature for Co-doped compounds $Co_xTi_{1-x}S_2$ with (a) $x = 0$, (b) $x = 0.05$, (c) $x = 0.10$, (d) $x = 0.20$, and (e) $x = 0.30$.

previous results reported by Klipstein et al.[32] In contrast, the ρ–T curves for the doped compounds ($x = 0.05$, 0.10, and 0.20) show semiconductor-like behavior (i.e., $d\rho/dT < 0$) as temperature decreases to a critical temperature T_c (= 22.6 K, 14.9 K, and 10.0 K for $x = 0.05$, 0.10, and 0.20, respectively), although they still exhibit metal-like behavior in high-temperature regions, similar to the phenomenon observed in the substituted compounds $Mg_xTi_{1-x}S_2$.[29] This is quite contrary to the case of the purely intercalated compounds M_yTiS_2, whose metallic behavior enhances with increasing intercalated element content.[24,33,34] In addition, T_c was found to decrease with increasing Co content for $x < 0.30$; however, when x reaches 0.30, the resistivity behaves metallically over the whole temperature range investigated and no critical temperature T_c is observed.

The reason why $Co_xTi_{1-x}S_2$ transitions from metallic behavior ($x = 0$) to semiconducting behavior ($0 < x < 0.30$) after substitution may lie in the fact that TiS_2 is a semiconductor with a narrow band gap.[11] However, in practice, self-intercalation of Ti into TiS_2 is unavoidable in the synthesis process.[28] As a result, TiS_2 almost always appears as an extrinsic semiconductor. Moreover, if the ionization energy of self-intercalated Ti atoms is small enough, complete ionization will occur at the low temperatures that can normally be reached. If the number of intercalated Ti atoms (acting as donors) is sufficiently large, a degenerate semiconductor that behaves metallically will form, as observed normally in TiS_2. As Co^{3+} is substituted for Ti^{4+}, acceptors (Co^{3+}) will be introduced. Then, the electron concentration will decrease if compensation takes place. Consequently, when the Co content (number of acceptors) is high enough, de-degeneration of TiS_2 will occur, leading to the appearance of semiconductor behavior. These results suggest that intercalation and substitution exist simultaneously in these Co-doped compounds. Hence, the appearance of semiconductor-like behavior means that substitution of Co for Ti plays a major role in the lightly doped compounds. However, with increasing Co content x, the number of intercalated Co atoms becomes greater, leading to metal-like behavior and the formation of a typical degenerate semiconductor[29] for $x = 0.30$.

Effects of Co Doping on Thermopower

The variations of the Seebeck coefficient (S) for $Co_xTi_{1-x}S_2$ with temperature are shown in Fig. 5. The negative values of the Seebeck coefficient found for all of the specimens over the entire temperature range show that the major charge carriers in $Co_xTi_{1-x}S_2$ are electrons. Moreover, one can see from Fig. 5 that the Seebeck coefficients of the Co-doped compounds $Co_xTi_{1-x}S_2$ ($x > 0$) are smaller than that of pure TiS_2. The absolute thermopower decreased with increasing Co content x in slightly doped compounds ($0 < x < 0.10$); however, for $x = 0.10$, the absolute thermopower of $Co_{0.1}Ti_{0.9}S_2$ was larger than that of slightly doped compounds ($0 < x < 0.10$), and for $x \geq 0.10$, the absolute thermopower of such heavily doped compounds also decreased with increasing Co content x.

The temperature behavior of the Seebeck coefficient for the doped compounds $Co_xTi_{1-x}S_2$ ($x > 0$) with different Co contents is more or less similar to that of pure TiS_2: the absolute thermopower for every compound was found to increase continuously with increasing temperature over the whole temperature range investigated. The small valley observed at a temperature around 60 K for each of them in the plot of S versus T could be ascribed to the phonon-drag effect.[30] At temperatures above 80 K, the thermopower for $Co_xTi_{1-x}S_2$ exhibited an

Table II. Slope of the plot of S versus T and E_F calculated from Eq. (1)

x	0	0.05	0.10	0.20	0.30
Slope (μV/K^2)	−0.6242	−0.4352	−0.5005	−0.4227	−0.3463
E_F (eV)	0.118	0.1692	0.1472	0.1743	0.2127

approximately linear relationship with temperature. The diffusive part of the thermopower (T-linear thermopower) can be described by the following formula:[30]

$$S = \frac{\pi^2 k^2 T}{eE_F,} \quad (1)$$

where k and e are the Boltzmann constant and the electron charge, respectively. This formula indicates that the slope of the plot of S versus T is inversely proportional to the Fermi level. Hence, the decrease in the slope of the plot of S versus T reflects the increase in E_F (or increase in electron concentration) due to Co intercalative doping, which can explain why the absolute thermopower $|S|$ decreases with Co doping, as shown in Fig. 5. The best fit of the data to Eq. (1) enables estimation of the Fermi level E_F for all the compounds, as presented in Table II. One can see that E_F increased from 0.118 eV for $x = 0$ to 0.2127 eV for $x = 0.30$ except for $x = 0.1$. This increase of E_F is a reflection of the increasing electron concentration.

Effects of Co Doping on Thermal Conductivity

The temperature dependence of the total thermal conductivity κ for the $Co_xTi_{1-x}S_2$ materials is shown in Fig. 6. It can be seen that Co substitution for Ti causes an increase in the thermal conductivity. Similar to the case of TiS_2, the thermal conductivity κ of the doped compounds shows a weak temperature dependence above 70 K, below which κ of all the compounds increases rapidly and approximately linearly with increasing temperature. The total thermal conductivity κ can be expressed as the sum of a lattice component (κ_l) and an electronic component (κ_e) as $\kappa = \kappa_l + \kappa_e$. κ_e values can be estimated from the Wiedemann–Franz law as $\kappa_e = LT/\rho$ (here L is the Lorenz number, and $L = 2.44 \times 10^{-8}$ V^2/K^2 for free electrons). Consequently, κ_L can be obtained from κ and κ_e, as shown in Fig. 7. Comparing Figs. 6 with 7, it can be seen that the values and temperature dependences of the lattice conductivity κ_l are similar to those of the total thermal conductivity κ. This result indicates that the thermal conductivity of $Co_xTi_{1-x}S_2$ comes mainly from the lattice conductivity, and generally Co doping causes an increase in the lattice thermal conductivity of $Co_xTi_{1-x}S_2$. The lattice conductivity κ_l can be expressed as $\kappa_l = 1/3C_v \cdot v \cdot l$ (here C_v is the specific heat, v is the acoustic velocity, and l is the mean free path of phonons). Since the mean free path of phonons l usually becomes smaller due to point defect

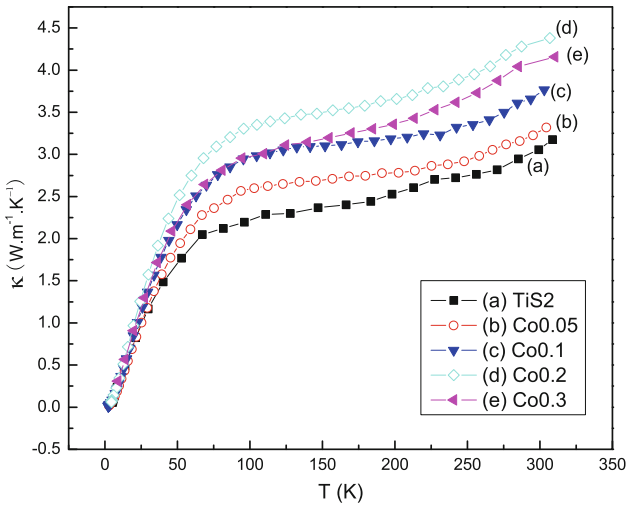

Fig. 6. Thermal conductivity κ versus temperature for the Co-doped compounds $Co_xTi_{1-x}S_2$ with (a) $x = 0$, (b) $x = 0.05$, (c) $x = 0.10$, (d) $x = 0.20$, and (e) $x = 0.30$.

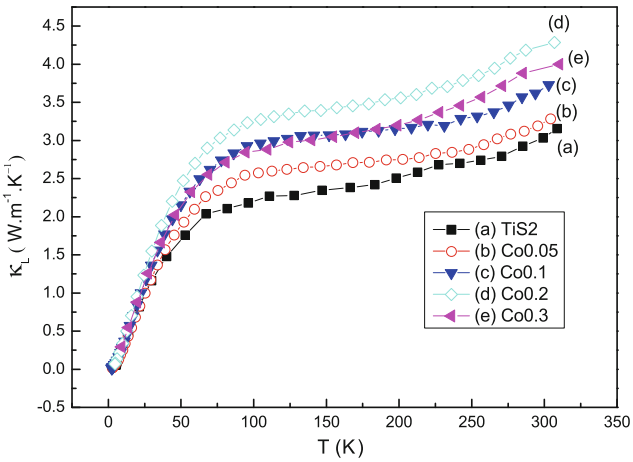

Fig. 7. Lattice thermal conductivity κ_L versus temperature for the Co-doped compounds $Co_xTi_{1-x}S_2$ for (a) $x = 0$, (b) $x = 0.05$, (c) $x = 0.10$, (d) $x = 0.20$, and (e) $x = 0.30$.

scattering after doping and the specific heat will not change strongly as the dopant content is not high, the enhancement of lattice thermal conductivity after Co doping could originate from an increase in the acoustic velocity due to enhancement of chemical bonds in the doped compounds, which seems to be supported by the decrease of the parameters a and c after Co doping (Fig. 3). Specifically, accompanying Co substitution for Ti, cobalt

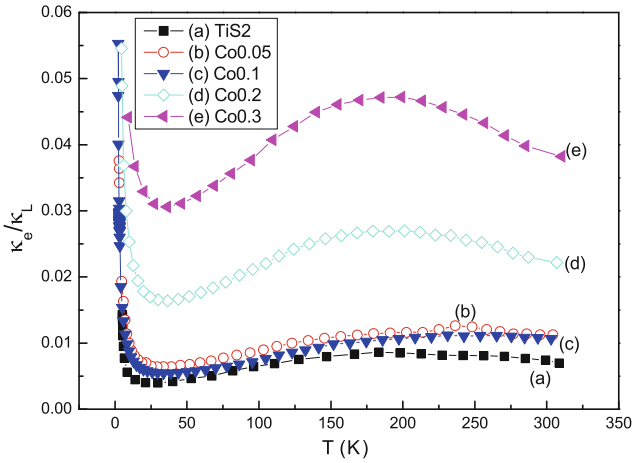

Fig. 8. The ratio κ_e/κ_L versus temperature for $Co_xTi_{1-x}S_2$ with (a) $x = 0$, (b) $x = 0.05$, (c) $x = 0.10$, (d) $x = 0.20$, and (e) $x = 0.30$.

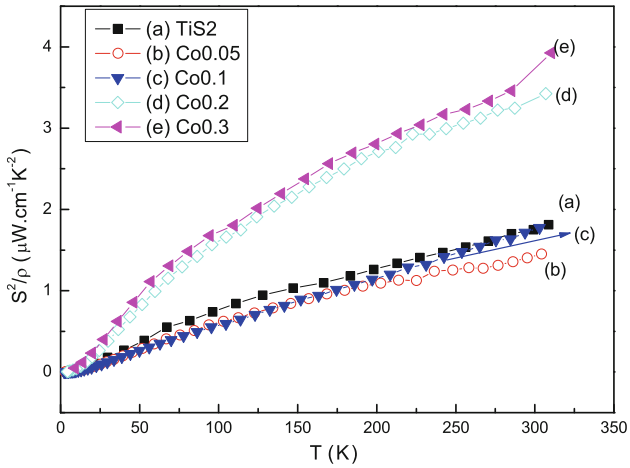

Fig. 9. Dependence of the power factor (S^2/ρ) on temperature for $Co_xTi_{1-x}S_2$ with (a) $x = 0$, (b) $x = 0.05$, (c) $x = 0.10$, (d) $x = 0.20$, and (e) $x = 0.30$.

intercalation occurred, leading to the formation of S-Co bonds among the intercalated Co atoms and S atoms (in the S-Ti-S sheet), bridging the van der Waals gaps, which will give rise to substantial strengthening of chemical bonds of the overall assembly and therefore the increase of the acoustic velocity. We can see from Fig. 8 that the ratio κ_e/κ increased with increasing Co content x. These results indicate that the electron concentration increased along with the level of Co doping, which agrees with the relationship between electronic conductivity and Co content x of the doped compounds $Co_xTi_{1-x}S_2$ (Fig. 4).

Effects of Co Substitution on Thermoelectric Properties

The power factor (S^2/ρ) is plotted as a function of temperature for all the samples in Fig. 9. One can see from Fig. 9 that the power factor of the slightly doped compounds $Co_xTi_{1-x}S_2$ ($x \le 0.10$) is smaller than that of pure TiS_2 due to the considerable decrease in thermopower. However, the power factor of the heavily doped compound $Co_{0.3}Ti_{0.7}S_2$ significantly exceeds that of pure TiS_2 over the whole measured temperature range, reaching 3.93 μW/cm K^2 at 310 K, which is about 117% larger than that (1.81 μW/cm K^2) of TiS_2.

Figure 10 shows the temperature dependence of the dimensionless figure of merit ZT (= $TS^2/\rho\kappa$) for TiS_2 and the Co-doped compounds $Co_xTi_{1-x}S_2$. The ZT value for all the specimens increases with increasing temperature. However, the ZT of slightly doped compounds ($x \le 0.10$) is smaller than that of pure TiS_2 because of the large increase in their thermal conductivity and decrease in thermopower, although their electronic resistivity decreases considerably. Nevertheless, the ZT value of the heavily doped compound $Co_{0.3}Ti_{0.7}S_2$ surpasses that of pure TiS_2 over the whole temperature range investigated,

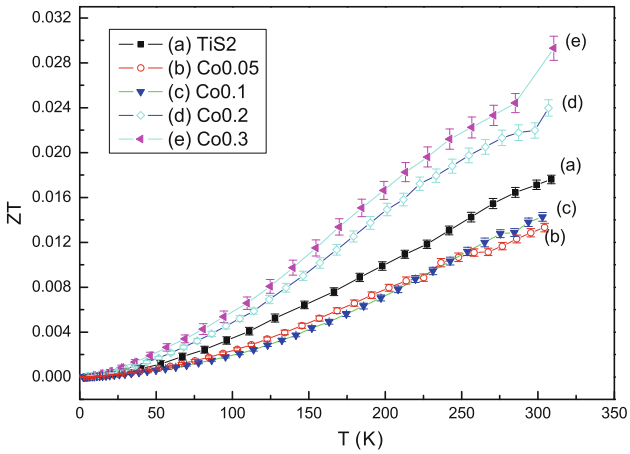

Fig. 10. Variation of ZT with temperature for Co-doped compounds $Co_xTi_{1-x}S_2$ with (a) $x = 0$, (b) $x = 0.05$, (c) $x = 0.10$, (d) $x = 0.20$, and (e) $x = 0.30$.

increasing rapidly with increasing temperature. Specifically, the ZT value of $Co_{0.3}Ti_{0.7}S_2$ reaches 0.0293 at 310 K, which is about 1.7 times as large as that of TiS_2 (ZT = 0.0176), demonstrating a spectacular improvement of thermoelectric performance for the proper Co doping content. The ZT value achieved by Co doping at room temperature is relatively small compared with that of state-of-the-art thermoelectric materials (for example, Bi_2Te_3); however, our research offers an approach to enhance the thermoelectric performance of materials with similar crystal structures to that of TiS_2.

CONCLUSIONS

We have studied the effect of Co doping on the thermoelectric properties of $Co_xTi_{1-x}S_2$. The results indicated that a transition from metal-like to semiconductor-like behavior occurred with Co doping. This transition implies that TiS_2 is a degenerate

semiconductor, which would be de-degenerated by a reduction in electron concentration due to Co substitution for Ti. The absolute thermopower $|S|$ and the resistivity were found to decrease significantly over the whole temperature range investigated, which can mainly be ascribed to an increase of electron concentration due to intercalation of Co atoms. The increase of lattice thermal conductivity of the doped compounds may be caused by enhanced acoustic velocity due to the formation of Co-S bonds between intercalated Co atoms and S atoms in the S-Ti-S sheet, bridging the van der Waals gap. The figure of merit, ZT, of the heavily doped compound $Co_{0.3}Ti_{0.7}S_2$ was improved over the whole temperature range investigated compared with that of TiS_2, reaching 0.0293 at 310 K, which is about 1.7 times as large as that of TiS_2, indicating that Co doping is an effective approach to enhance the thermoelectric performance of TiS_2.

ACKNOWLEDGEMENTS

Financial support from the National Natural Science Foundation of China (Nos. 10904144, 50972146, and 50701043) is gratefully acknowledged.

REFERENCES

1. V.V. Ivanovskaya and G. Seifert, *Solid State Commun.* 130, 175 (2004).
2. P.C. Klipstein and R.H. Friend, *J. Phys. C* 17, 2713 (1984).
3. D.L. Greenway and R.T. Nitsche, *Phys. Chem. Solids* 26, 1445 (1965).
4. C.H. Chen, W. Fabian, F.C. Brown, K.C. Woo, B. Davies, B. DeLong, and A.H. Thompson, *Phys. Rev. B* 21, 615 (1980).
5. J.J. Barry, H.P. Hughes, P.C. Klipstein, and R.H. Friend, *J. Phys. C* 16, 393 (1983).
6. F.R. Shepherod and P.M. Williams, *J. Phys. C* 7, 4416 (1974).
7. D.R. Allan, A.A. Kelsey, S.J. Clark, R.J. Angel, and G.J. Ackland, *Phys. Rev. B* 57, 5106 (1998).
8. G.A. Benesh, A.M. Woolley, and C. Umrigar, *J. Phys. C* 13, 1595 (1985).
9. C.M. Fang, R.A. de Groot, and C. Haas, *Phys. Rev. B* 56, 4455 (1997).
10. Z.Y. Wu, G. Ouvrard, S. Lemaux, P. Moreau, P. Gressier, F. Lemoigno, and J. Rouxel, *Phys. Rev. Lett.* 77, 2101 (1996).
11. Z.Y. Wu, F. Lemoigno, P. Gressier, G. Ouvrard, P. Moreau, J. Rouxel, and C.R. Natoli, *Phys. Rev. B* 54, R11009 (1996).
12. Z.Y. Wu, G. Ouvrard, P. Moreau, and C.R. Natoli, *Phys. Rev. B* 55, 9508 (1997).
13. S. Sharma, T. Nautiyal, G.S. Singh, S. Auluck, P. Blaha, and C. Ambrosch-Draxl, *Phys. Rev. B* 59, 14833 (1999).
14. A.H. Reshak and S. Auluck, *Phys. Rev. B* 68, 245113 (2003).
15. E.E. Abbott, J.W. Kolis, N.D. Lowhorn, W. Sams, and T.M. Tritt, *Mater. Res. Soc. Symp. Proc.* 793, 295 (2004).
16. C.A. Kukkonen, W.J. Kaiser, E.M. Logothetis, B.J. Blumenstock, P.A. Schroeder, S.P. Faile, R. Colella, and J. Gambold, *Phys. Rev. B* 24, 1691 (1981).
17. M.S. Whittingham, *Prog. Solid State Chem.* 12, 41 (1978).
18. Z. Mao and R.E. White, *J. Power Sources* 43, 181 (1993).
19. P.G. Bruce and M.Y. Saidi, *J. Electroanal. Chem.* 322, 93 (1992).
20. A.H. Thompson, *Phys. Rev. L* 40, 1511 (1978).
21. C.M. Julien, *Mater. Sci. Eng. R* 40, 47 (2003).
22. K. Suzuki, O. Nakamura, T. Kondo, and T. Enoki, *J. Phys. Chem. Solids* 57, 1133 (1996).
23. H. Imai, Y. Shimakawa, and Y. Kubo, *Phys. Rev. B* 64, 241104(R) (2001).
24. D. Li, X.Y. Qin, J. Zhang, L. Wang, and H.J. Li, *Solid State Commun.* 135, 237 (2005).
25. D. Li, X.Y. Qin, J. Liu, and H.S. Yang, *Phys. Lett. A* 328, 493 (2004).
26. J. Zhang, X.Y. Qin, D. Li, and H.Z. Dong, *J. Phys. D Appl. Phys.* 39, 1230 (2006).
27. E.W. Ong, M.J. McKelvy, G. Ouvrard, and W.S. Glaunsinger, *Chem. Mater.* 4, 14 (1992).
28. H. Kobayashi, K. Sakashita, M. Sato, T. Nozue, T. Suzuki, and T. Kamimura, *Physica B* 169–171, 237 (1997).
29. X.Y. Qin, J. Zhang, D. Li, and H.Z. Dong, *J. Appl. Phys.* 102, 073703 (2007).
30. J. Zhang, X.Y. Qin, D. Li, H.X. Xin, L. Pan, and K.X. Zhang, *J. Alloy Compd.* 479, 816 (2009).
31. A.N. Titov, A.V. Kuranov, V.G. Pleschev, Y.M. Yarmoshenko, M.V. Yablonskikh, A.V. Postnikov, S. Plogmann, M. Neumann, A.V. Ezhov, and E.Z. Kurmaev, *Phys. Rev. B* 63, 035106 (2001).
32. P.C. Klipstein, A.G. Bagnall, W.Y. Liang, E.Z. Marseglia, and R.H. Frend, *J. Phys. C Solid State Phys.* 14, 4067 (1981).
33. P.C. Klipstein and R.H. Friend, *J. Phys. C: Solid State Phys.* 20, 4169 (1987).
34. C. Julien, I. Samaras, O. Gorochov, and A.M. Ghorayeb, *Phys. Rev. B* 45, 13390 (1992).